Real-time analysis of double-strand DNA break repair by homologous recombination

Wade M. Hicks, Miyuki Yamaguchi, and James E. Haber[1]

Department of Biology and Rosenstiel Basic Medical Sciences Center, Brandeis University, Waltham, MA 02454-9110

This contribution is part of the special series of Inaugural Articles by members of the National Academy of Sciences elected in 2010.

Contributed by James E. Haber, January 5, 2011 (sent for review November 23, 2010)

The ability to induce synchronously a single site-specific double-strand break (DSB) in a budding yeast chromosome has made it possible to monitor the kinetics and genetic requirements of many molecular steps during DSB repair. Special attention has been paid to the switching of mating-type genes in *Saccharomyces cerevisiae*, a process initiated by the HO endonuclease by cleaving the *MAT* locus. A DSB in *MAT*a is repaired by homologous recombination—specifically, by gene conversion—using a heterochromatic donor, *HML*α. Repair results in the replacement of the a-specific sequences (Ya) by Yα and switching from *MAT*a to *MAT*α. We report that *MAT* switching requires the DNA replication factor Dpb11, although it does not require the Cdc7-Dbf4 kinase or the Mcm and Cdc45 helicase components. Using Southern blot, PCR, and ChIP analysis of samples collected every 10 min, we extend previous studies of this process to identify the times for the loading of Rad51 recombinase protein onto the DSB ends at *MAT*, the subsequent strand invasion by the Rad51 nucleoprotein filament into the donor sequences, the initiation of new DNA synthesis, and the removal of the nonhomologous Y sequences. In addition we report evidence for the transient displacement of well-positioned nucleosomes in the *HML* donor locus during strand invasion.

yeast mating type switching | DNA repair kinetics | nucleosome displacement | *MAT* switching

The integrity of eukaryotic chromosomes is under constant assault from a variety of DNA-damaging agents, the most severe being double-strand breaks (DSBs). DSBs can arise from a number of exogenous agents; however the principal source of DSBs is the process of DNA replication itself (1). In vertebrate cells, there can be 10 or more such DSBs every replication cycle requiring homologous recombination (HR) machinery for repair.

DSBs are repaired by two major processes: nonhomologous end-joining (NHEJ) and HR; both include several different mechanisms. In budding yeast, NHEJ repair of an HO endonuclease-induced DSB, which has 4-bp 3′ overhanging ends, can occur either via an error-free mechanism that simply relegates overhanging broken ends to restore the original sequences, or by several error-prone mechanisms that anneal one or a few base pairs in the overhanging regions to produce small deletions or templated insertions (2). Studying yeast also provided early evidence of an "alternative NHEJ" mechanism called microhomology-mediated end-joining (MMEJ) (3). NHEJ and MMEJ are especially important in G1 cells before chromosomal replication and thus before a lesion on one sister chromatid can be repaired by HR; but NHEJ/MMEJ can occur throughout the cell cycle (2).

When one or both DSB ends share homology to other genomic sequences (a sister chromatid, a homologous chromosome, or a segment located ectopically), repair can occur by HR. Four major mechanisms have been described: single-stranded annealing (SSA), break-induced replication (BIR), and two types of gene conversion (GC): double Holliday junction intermediate (dHJ) pathway, which can result in crossover (CO) products, and synthesis-dependent strand annealing (SDSA), in which COs are rare. All HR types rely on proteins belonging to the *RAD52* epistasis group. They all require Rad52 protein, and most require Rad51 recombinase and associated proteins Rad54, Rad55, and Rad57 (4).

A detailed understanding of these DSB repair mechanisms has relied on the ability to induce a single site-specific DSB in a budding yeast chromosome. One can follow the appearance of intermediates and products by physically monitoring changes in DNA fragments, using Southern blots or PCR assays. In yeast, this kind of analysis was first done to analyze nonreciprocal exchange (GC) of homing intron DNA in mitochondria (5) and kinetics of meiotic CO formation (6). Soon thereafter it became possible to explore repair in chromosomes of mitotic cells by taking advantage of HO and I-SceI site-specific endonucleases to create unique DSBs. In 1988 we began these studies, investigating both SSA and GC (7–9), especially the GC process for which HO endonuclease apparently evolved: mating-type (*MAT*) gene switching (10).

Mating type in *Saccharomyces cerevisiae* is dictated by two alleles, *MAT***a** or *MAT*α, which differ from each other in the 650-bp Y**a** or 700-bp Yα regions that contain the promoters and most of the coding regions of *MAT***a***1* and *MAT***a***2* or *MAT*α*1* and *MAT*α*2*, respectively (Fig. 1*A*). *MAT* shares homology with two other sites located near the telomeres of the same chromosome, *HML*α and *HMR***a**. Both donors have complete copies of the mating-type genes, but these are kept silent in heterochromatin by the combined action of cis-acting silencer sequences and recruitment of the Sir2/Sir3/Sir4 histone deacetylase complex (reviewed in refs. 11 and 12). *MAT* switching is initiated by site-specific HO cleavage of the single accessible site in the yeast genome at *MAT*; highly positioned nucleosomes at the donor loci prevent cleavage (13). When *MAT***a** switches using *HML*α as the donor, the DSB end to the right of the cut is fully homologous to a 327-bp Z1 and Z2 region in *HML*, whereas the left side ssDNA begins with 650 nt of nonhomologous (NH)-Y**a** sequence before *MAT* sequences encounter approximately 1,400 bp of homology (the W and X regions). *MAT*α shares less homology with *HMR***a** on both sides (X and Z1 only), but switching is equally efficient. Repair is highly biased so that *MAT***a** cells recombine preferentially with *HML*α and *MAT*α cells with *HMR***a** (14–16), controlled by the cis-acting Recombination Enhancer (RE).

Normally, *HO* is under strict cell cycle and cell lineage control, but creation of a galactose-inducible *HO* gene (17) made it possible to synchronously cleave *MAT* in a large cell population. When we followed the fate of broken DNA ends by Southern blot analysis, we were somewhat surprised to find that *MAT***a** switching in cycling cells takes at least 1 h from the time a DSB is detected until the appearance of a new restriction fragment indicative of *MAT*α (18). Subsequent experiments showed there were a number of slow steps (Fig. 1*B*). DSB repair depends on 5′ to 3′ resection of DSB ends, at a rate of approximately 1 nt/s

Author contributions: W.M.H., M.Y., and J.E.H. designed research; W.M.H. and M.Y. performed research; W.M.H. and M.Y. contributed new reagents/analytic tools; W.M.H., M.Y., and J.E.H. analyzed data; and W.M.H. and J.E.H. wrote the paper.

The authors declare no conflict of interest.

[1]To whom correspondence should be addressed. E-mail: haber@brandeis.edu.

This article contains supporting information online at www.pnas.org/lookup/suppl/doi:10.1073/pnas.1019660108/-/DCSupplemental.

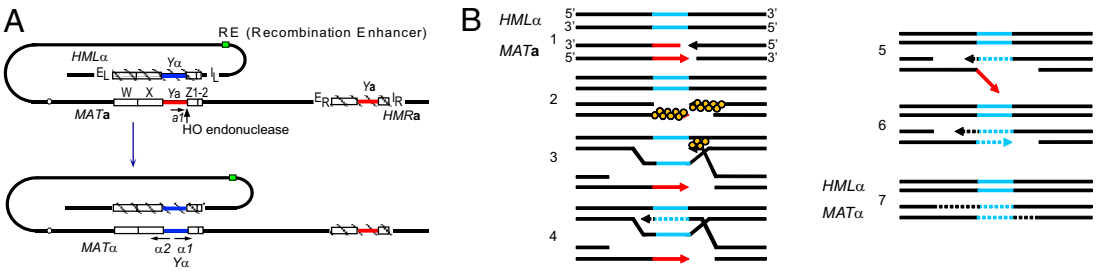

Fig. 1. Schematic of *S. cerevisiae* mating type loci on chromosome III and the SDSA model of *MAT* switching. (*A*) Chromosome III contains three mating type genes, the expressed *MAT locus* and *HML* and *HMR*, which are heterochromatic and silent. *MAT***a** cells switch using *HML*α, whereas *MAT*α cells recombine with *HMR***a**. This preference is controlled by the RE element. (*B*) Individual steps of the DSB repair mechanism are numbered on the left. 1: *MAT* switching is initiated by an HO-induced DSB at the Ya-Z1 junction within *MAT***a**. 2: 5′–3′ resection creates ssDNA with 3′ ends to which Rad51 (yellow circles) is recruited. 3: The Rad51 filament searches for homologous dsDNA. 4: Upon *MAT-HML* synapsis, new DNA synthesis is primed from the free 3′ end of the invading strand. 5: The nascent strand is dissociated from the donor and anneals with homologous sequences on the left side of the break. 6: The nonhomologous 3′ tail is clipped off, and new DNA synthesis begins at the free 3′ ends to fill in the single-stranded gaps. 7: DSB repair is completed by ligation of the filled-in ends. In the SDSA model, all newly synthesized DNA appears at the repaired locus, whereas the donor locus remains unmodified.

(19), to create long 3′-ended ssDNA that recruits Rad51 recombinase, which in turn initiates a search for homologous donor sequences. Resection depends on the activity of cell division kinase 1, Cdc28; thus in G1-arrested cells, when Cdc28 is inactive, DSBs are primarily repaired by NHEJ (20, 21). Homology searching results in formation of a stand-invasion intermediate [a displacement loop (D-loop)] that allows for initiation of new DNA synthesis, which copies one strand coding the opposite mating-type information. Initiation of DNA synthesis can be monitored by a PCR assay using one primer in Yα sequences at *HML* and one distal to *MAT*, allowing amplification of a unique template created after at least 26 nt of new DNA are copied from *HML*α (18). This first strand is then apparently displaced from the donor and used as a template to copy the second strand, initiated by annealing W and X sequences on the second DSB end and after NH-Y sequences are removed.

The development of ChIP made it possible to determine which proteins were associated with *MAT* and donor loci during DSB repair. ssDNA ends first become bound by replication factor A (RPA), a single-strand DNA binding protein complex, which is displaced during Rad51 nucleoprotein filament assembly (22). ChIP also allowed us to see the next important step in repair: association of the Rad51 filament with the donor locus. Thus, when anti-Rad51 antibody pulled down DNA cross-linked to Rad51, we saw that Rad51 became associated with the ssDNA end much sooner than when it encountered donor DNA (23, 24).

Switching culminates in replacement of the Y sequences and reestablishment of unbroken chromatin at *MAT*. Whereas the classic DNA density labeling experiment of Meselson and Stahl (25) demonstrated that normal DNA replication was semiconservative, when we used this technique to study *MAT* switching we found both newly copied strands at *MAT*; the donor was unaltered (26). This study confirmed the conclusion drawn from a number of experiments suggesting that *MAT* switching occurs predominantly through SDSA, in which there would be little or no associated CO (reviewed in ref. 27). COs do appear at a low frequency, as revealed by creation of a deletion between *MAT* and *HMR* or a circular chromosome fusing *MAT* and *HML* (28–30). Intermediates consistent with the observation of a low level of dHJ intermediates during mitotic GC have also been observed using the site-specific endonuclease I-SceI (31).

Although these intermediate steps in DSB-induced mitotic recombination have been identified, most analyses were carried out with intervals of 30 min or more, making it difficult to describe the process in fine detail. Moreover, many early experiments used a *GAL::HO* gene carried on a plasmid, so that a significant fraction of cells lost the plasmid by the time *HO* was induced and did not undergo recombination. In addition, some steps that must take place during *MAT* switching were never examined, such as the timing of NH-Y tail clipping or the role the left side of the break plays in the repair process. Moreover there was no analysis of changes in the *HML* donor heterochromatic structure.

Here we report a detailed kinetic analysis of many important steps during DSB repair. In some of these experiments we used a modified strain in which both the left and right sides of the DSB are equally homologous to the donor. Other experiments use a strain modified such that only the right side of a DSB at *MAT* shares homology with the donor. Taken altogether the results reported herein give us a clearer picture of the sequence of events that occur during DSB repair and raise new questions for future exploration.

Results

High-Resolution Kinetic Analysis of the Intermediate Steps of *MAT* Switching. To improve the resolution of early steps in *MAT* switching, samples were collected at 10-min intervals over 1.5 h from the time of HO induction. Kinetics were measured in strain JKM161 (*HML*α *MAT***a** *hmr*Δ), carrying a *GAL::HO* gene integrated at the *ADE3* locus (23). Quantitative Southern blot analyses show *MAT***a** is cleaved in nearly 100% of the cells 20 min after inducing HO expression; 50% show DSB formation in 10 min (Fig. 2*A*). DSB repair completion is initially seen 70 min after HO induction. As described below, this hour-long delay consists of a number of kinetically slow steps.

To assay intermediate repair steps we made use of ChIP using anti-Rad51 antibodies. We define the initiation point for each step as the time at which the ChIP signal is statistically significantly greater than the initial background level. Rad51 recruitment to the *Z*-regions at *MAT* begins 20 min after *HO* induction (Fig. 2*B*). Thus, 5′ to 3′ resection sufficient to load Rad51 must occur very rapidly after DSB formation, although there is a delay that we have previously attributed to sequential loading first of RPA and then its Rad52-mediated replacement by Rad51 (22). Rad51 starts to appear at the 5′ end of the W region, ≈2 kb away from the HO cut site on the left side of *MAT*, 30 min after HO induction, consistent with the resection rate (Fig. 2*B*).

After Rad51 recruitment to *MAT*, the nucleoprotein filament searches the genome for homologous sequences. ChIP experiments can also determine the timing of Rad51 interaction with *HML* donor sequences, reflecting strand invasion. Rad51 was detected at *HML* 10 min after Rad51 was observed at *MAT* (Fig. 2*C*). Interestingly, Rad51 association with the 5′ end of *HML*-W, reflecting stand invasion of the W/X regions on the left side of the DSB, was greatly delayed and reached levels much lower than that seen for *HML*-Z (Fig. 2*C*). Although the W regions of *MAT* and *HML* do not seem to interact as rapidly as do the Z regions, it is still possible that homologous sequences closer to the 3′ end of the homologous X regions do synapse but cannot be detected using ChIP PCR primers at the 5′ end of the W region,

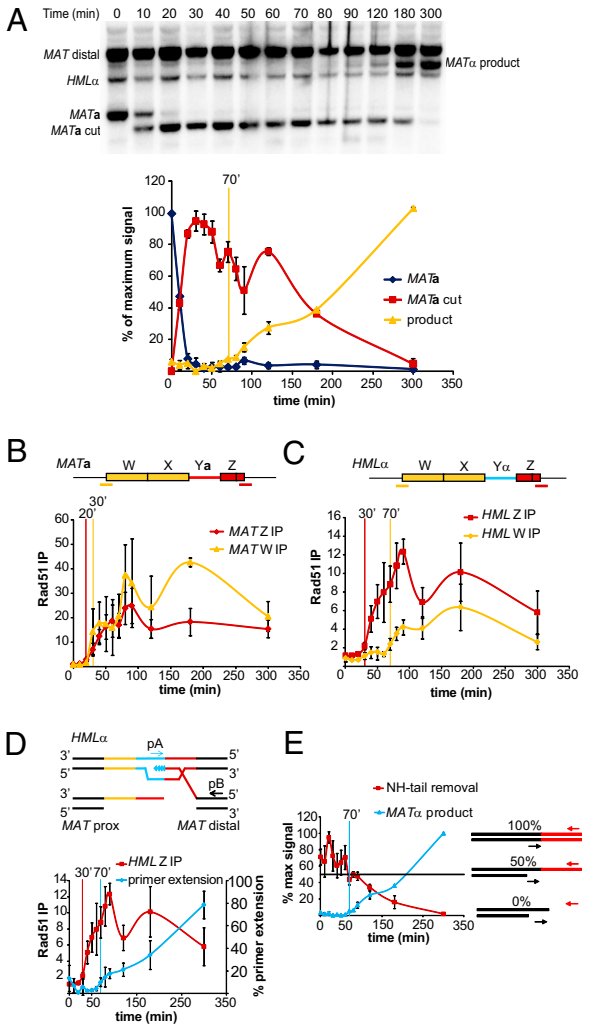

Fig. 2. High-resolution kinetics of *MAT***a** switching to *MAT*α. (*A*) Representative Southern blot showing *MAT* switching progression. Purified gDNA was digested with StyI. Graph shows quantitative densitometric analysis from two independent experiments; error bars represent ranges. Vertical yellow bar indicates the time point at which product formation becomes detectable over background. (*B*) Rad51 ChIP analysis at *MAT***a**. (*C*) Rad51 ChIP analysis at *HML*α. Red and yellow bars underneath the *MAT***a** and *HML*α denote positions of primer pairs used to detect Rad51 recruitment to these regions. Rad51 ChIP data were normalized to *ARG5,6*. Each ChIP experiment represents four independent experiments; error bars indicate SEM. (*D*) Schematic of primer extension assay and a comparison of Rad51 ChIP to *HML* Z-region and primer extension, from four independent experiments; error bars indicate SEM. Vertical bars in *B–D*, colored respectively for each data set, indicate the time at which ChIP or primer extension signals become significantly different from T_0 (*t* test, $P < 0.05$). (*E*) Schematic of NH-tail clipping assay and a comparison of NH-tail clipping and primer extension kinetics. The horizontal black line denotes the 50% level. Data from four independent experiments; error bars indicate SEM.

1.4 kb away. To address the role of the left side of the DSB, we modified *HML*, as described in a later section.

After a successful homology search and strand-invasion with the donor, DNA synthesis is initiated. The DNA replication machinery that initiates new DNA synthesis requires only a subset of proteins needed for normal DNA replication or for recombination-induced, leading- and lagging-strand replication (BIR) (32–34). *MAT* switching does not require lagging-strand DNA polymerase-α, Mcm helicase proteins, or activation of replication by Cdc7 kinase. However, *MAT* switching does require Dpb11 (Fig. 3), which plays a key role during normal DNA

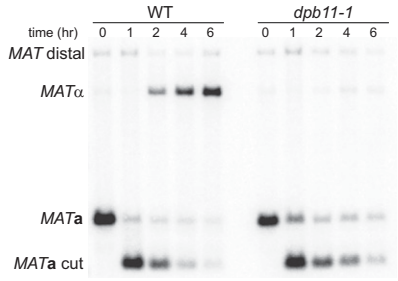

Fig. 3. Dpb11 is required for *MAT* switching. Southern blots show progression of *MAT***a** switching to *MAT*α after *cdc7-as3* arrest and shift to the 37 °C nonpermissive temperature (*Materials and Methods*). Purified gDNA was digested with StyI.

replication as part of a preloading complex of proteins at origins (35). To ensure that inactivating Dpb11 did not indirectly impair *MAT* switching by sequestering other replication proteins at stalled replication forks [as was the case when we analyzed DNA polymerase-α (33, 36)], we arrested temperature-sensitive *dpb11-1* cells (37) before DNA replication with an analog-sensitive *cdc7-as3* allele at 25 °C. The *dpb11-1* allele was then inactivated at 37 °C for 3 h before inducing HO expression. We have previously shown that blocking cells before S phase with cdc7-as3 does not impair *MAT* switching (20), allowing us to test the role of Dpb11 outside of its known role in initiating DNA replication. As shown in Fig. 3, inactivation of Dpb11 blocks completion of *MAT* switching. Thus, among DNA replication factors implicated in initiation of normal DNA replication, it seems that Dpb11, and presumably its associated Sld2 and Sld3 proteins, are required for initiation of repair DNA synthesis, which requires only leading-strand polymerases Polδ and/or Polε (33, 34).

To assay initiation of repair DNA synthesis, we used a PCR method that amplifies a unique product formed only after a small extent of new DNA synthesis has occurred (18) (Fig. 2*D*). Primer extension becomes apparent 70 min after HO induction, 40 min after initial detection of *MAT-HML* synapsis (Fig. 2*D*). Thus, initiation of repair associated DNA synthesis seems to be a major rate-limiting step, possibly reflecting the time required to assemble a competent replication machine. We have not yet assayed the timing of recruitment of proliferating cell nuclear antigen (PCNA) or DNA polymerases required for *MAT* switching.

The SDSA model imagines that the newly copied strand is displaced from the template much as RNA is extruded from DNA during transcription. For *MAT* switching to be completed, copying must extend from the synapsis site in Z to at least part of the way through *HML*-W/X such that the displaced single-stranded W/X sequences copied from *HML* can anneal to single-stranded, homologous W/X region on the left side of the DSB at *MAT* (Fig. 1*B*, step 5). After this strand annealing step, repair will be completed by a DNA polymerase extending the 3′ ends to fill in single-stranded gaps adjacent to *MAT*. Unless initial primer extension proceeds beyond the *HML*-W boundary, this end will be exactly homologous to *MAT*-W/X, allowing the 3′ end to be extended and fill in ssDNA generated by continuing 5′ to 3′ resection. However, similar to observations made in mammalian cells (38), we observed a PCR product consistent with synthesis beyond *HML*-W ≈1 to 2 h after HO induction. The proportion of cells that synthesize beyond the region of homology was not determined.

When the left-side (W-X-**Ya**) DSB end invades *HML*α it cannot effect primer extension and gap-filling until single-stranded **Ya** sequences, which are not homologous to the newly copied Yα region, are clipped off. This process requires Rad1–Rad10, Msh2–Msh3, Slx4, Saw1, and other components of a complex that can remove 3′-ended NH-tails in SSA and in *MAT* switching (39–43). To measure NH-tail clipping kinetics during *MAT* switching, we designed two PCR primers to anneal on either side of the *MAT*-X-**Ya** junction (Fig. 2*E*). In the absence of NH-tail clipping, quantitative PCR (qPCR) will measure

a 50% loss of template as resection renders the region single-stranded, but clipping off the NH-tail, which destroys the PCR template, will further decrease the PCR signal. NH-tail clipping and *MAT*α product formation occur coincidently, because NH-tail fragment concentrations did not decrease below 50% until 90–120 min, although some clipping must have occurred before this, considering that ≈5% of the population had completed repair by 70 min (Fig. 2*E*).

Modified System to Study the Role of the Left Side of the DSB, Containing Nonhomology, During *MAT* Switching. The weak and very late association of Rad51 with *HML*-W sequences was unexpected considering that homology to the left of the Y region is nearly five times larger than that on the right. One explanation for this lack of interaction is that the large NH-tail separating the free 3′ end of the DSB from homologous W/X sequences interferes with stable strand invasion. Rad51 filaments containing NH-tails might well synapse with homologous dsDNA, but these interactions would be unstable, because they cannot form topologically interwound plectonemic DNA structures without aid from a type I topoisomerase (44–46). However, it is also possible that ChIP PCR primers used to detect synapsis between *MAT*- and *HML*-W regions were too far away (1.4 kb) from the DSB end to detect *MAT-HML* pairing within the X region, just adjacent to the NH-Y**a** tail junction. This would be especially likely if Rad51 preferentially mediates strand exchange with a 5′–3′ polarity (47, 48).

To differentiate between a potentially unstable interaction caused by a protruding 3′ NH-tail or a decreased interaction at the 5′ end of the W region due to the polarity of Rad51-mediated strand exchange, all of W and most of X was deleted at *HML* so each side of a DSB at *MAT* shares the same amount of homology (327 bp) with *HML* (Fig. 4*A*). This construct [*HML*α(Δ327)] allowed us to position ChIP PCR primers closer to the 3′ end of X homology. This modification does not significantly affect the kinetics or efficiency of *MAT* switching as judged by primer extension and product formation (Fig. S1). In this strain, Rad51 is recruited to both the Z1–Z2 region and the truncated *HML*-X region 30–45 min after HO induction (Fig. 4*B*), indicating that the presence of an NH-tail does not prevent synapsis between *MAT-HML* X-regions and that our initial experiments failed to see this association because the *HML*-W region does not undergo Rad51-mediated strand invasion. This is consistent with the idea that Rad51 invades then extends strand invasion in a 5′ to 3′ direction, and also with studies showing that mutated sites in *HML*-X are transferred to *MAT* much more often than those in *HML*-W (49).

We note that NH-tail clipping must be able to occur at the point of *MAT-HML* synapsis because *MAT* switching is still reasonably efficient when both ends of the DSB contain terminal NH sequences (39, 50). This is further supported by the observation that *MAT* switching can give rise to reciprocal COs (28) thought to occur through a dHJ intermediate, whose formation would require NH-Y**a** tail clipping at the point of *MAT-HML* synapsis. To determine whether NH-tail clipping preferentially occurs at the point of *MAT-HML* synapsis or after the strand-annealing step of *MAT* switching (Fig. 1*B*, step 5), we measured NH-tail clipping in *rad54*Δ *rdh54*Δ cells, which are proficient for Rad51-mediated *MAT-HML* synapsis but cannot initiate primer extension (23, 51, 52). Previously we showed that Rdh54 plays no obvious role in *MAT* switching and that *rad54*Δ and *rad54*Δ *rdh54*Δ had identical phenotypes (23). Without Rad54 and Rdh54, PCR-amplifiable X-Y**a** junction DNA does not decrease below 50% (Fig. 5), indicating that these Swi/Snf proteins are required for NH-tail clipping. The requirement for Rad54 and Rdh54 could be that NH-tail clipping preferentially occurs after the SSA step, which requires repair-associated DNA synthesis, but this result could also be interpreted as requiring formation of a plectonemic structure at the point of *MAT-HML* synapsis, which in vitro has been shown to require Rad54 (53). As we show below, Rad54 allows synapsis between *MAT* and *HML* but fails to remodel chromatin, which may be an indication that only paranemic strand-pairing can occur without Rad54.

Modified *MAT* Switching System to Study Nucleosome Remodeling During Strand Invasion. Strand invasion into *HML* encounters an array of highly positioned nucleosomes, one of which (nucleosome L6) presumably prevents DSB formation at *HML* by excluding HO access. It was therefore of great interest to monitor nucleosome remodeling within *HML* heterochromatin during strand invasion. *MAT* switching experiments were designed on the basis of those used to monitor nucleosome remodeling at active promoters (54). We tiled PCR primers at *HML* such that known positions and boundaries of *HML*-specific nucleosomes (55, 56) could be easily identified after micrococcal nuclease (MNase) treatment (Fig. 6*A*).

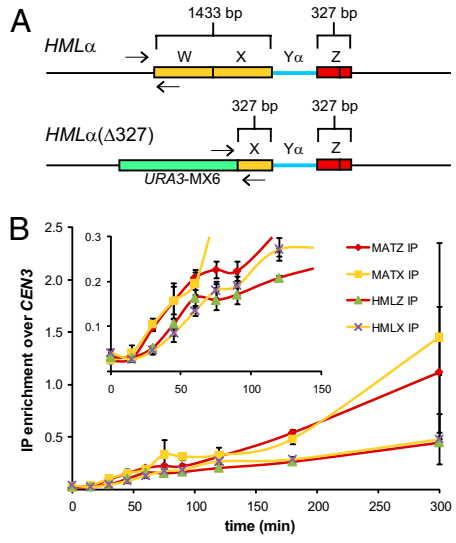

Fig. 4. Both sides of a DSB at *MAT* interact with homologous *HML* donor sequences. (*A*) Schematic of WT *HML* and *HML*(Δ327) showing the extent of homology shared with both sides of an HO-induced DSB at *MAT*. Arrows indicate PCR primer positions used to detect Rad51-mediated synapsis between the left side of a DSB at *MAT* and *HML*. (*B*) Kinetics of Rad51 ChIP to the indicated regions of *MAT* and *HML* during *MAT* switching in *HML*(Δ327) cells. *Inset:* Graph is enlarged part the larger graph to show differences in the timing of Rad51 recruitment to *MAT* and *HML*(Δ327). Rad51ChIP data are normalized to *CEN3*. Data represent three independent experiments; error bars indicate SEM.

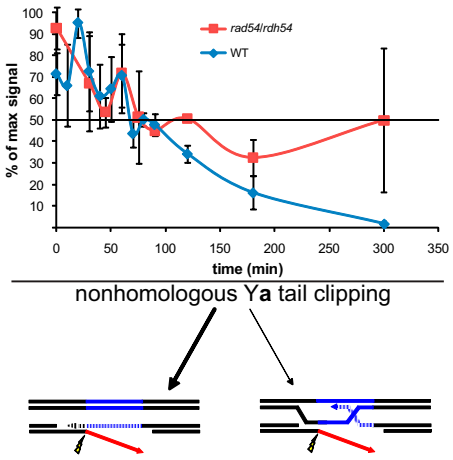

Fig. 5. Comparison of NH-tail clipping in *MAT* switching WT and *rad54*Δ/*rdh54*Δ (WH12) cells. Data from at least three independent *MAT* switching experiments; error bars indicate SEM.

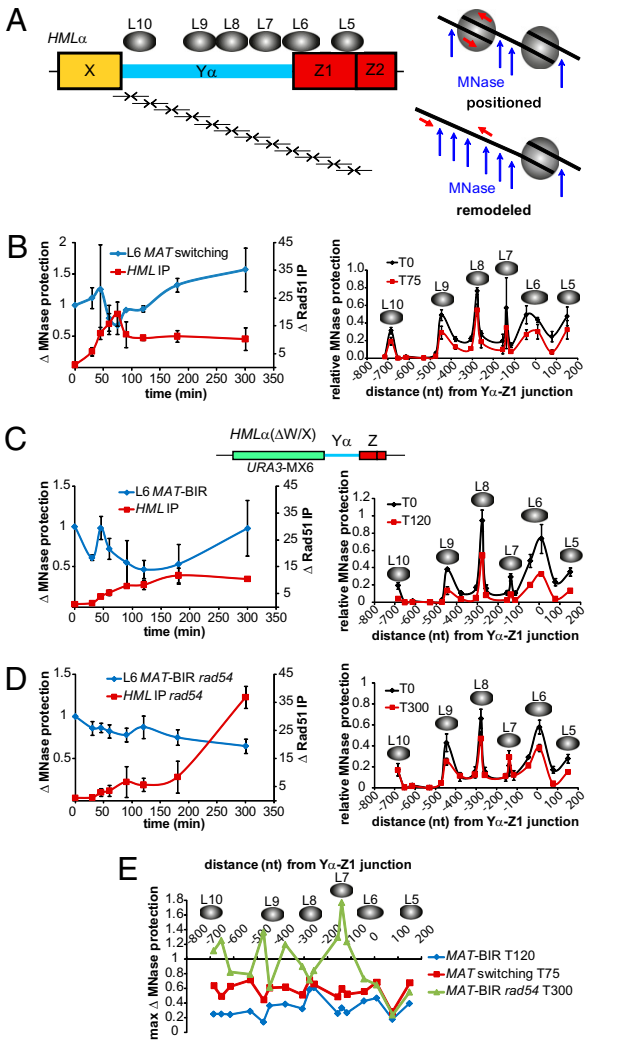

Fig. 6. Heterochromatic nucleosomes within *HML* are remodeled during *MAT* switching. (*A*) Nucleosome positions (gray ovals) at *HML* (56) and the MNase assay used to monitor changes in nucleosome positioning. Pairs of arrows below *HML* represent tiled primer pairs used to measure changes in MNase protection during *MAT* switching; not drawn to scale (see Table S1 for primer pairs and sequences). MNase only acts on DNA not bound by a nucleosome, therefore a primer pair positioned in a region bound by a nucleosome will amplify this DNA after MNase treatment. Any nucleosome remodeling will expose this DNA to MNase, resulting in a decrease in PCR signal. (*B–D*) Left graph compares Rad51 ChIP to *HML*, indicating *MAT-HML* synapsis, with changes in MNase protection for the L6 nucleosome, which is positioned over the HO recognition sequence at *HML*. Both Rad51 ChIP and L6 MNase protection data are plotted as fold changes from T_0. In *B*, the Rad51 ChIP data are normalized to *Arg5,6*, whereas in *C* and *D* data are normalized to *CEN3*. Right graph shows MNase protection across the *HML* region containing nucleosomes L5–L10 at 0 min (pre-HO induction) and the time after HO induction that showed the greatest decrease in MNase protection: 75, 120, and 300 min for (*B*) WT *HML* in WT cells (JKM161), (*C*) *HML*(ΔW/X) (*MAT*-BIR) in WT cells (WH219), and (*D*) *HML*(ΔW/X) (*MAT*-BIR) in *rad54::LEU2* cells (WH259), respectively. MNase protection levels are all relative to *Arg5,6* signals obtained from untreated samples for each respective time point. Data from thre independent experiments; error bars indicate SEM. (*E*) Comparison of the time after HO induction at which the maximum fold change in MNase protection within the *HML* region containing nucleosomes L5–L10 occurred for WT *MAT* switching, WT *MAT*-BIR, and *rad54::LEU2 MAT*-BIR.

The locations of *HML* nucleosomes L5–L10 before HO cleavage agree with previous data (55, 56) (Fig. 6 *B–D*). Because *MAT* also contains Z1 and Z2 regions, primers designed to detect the L5 nucleosome position as well as the internucleosomal region between L5 and L6 within *HML* could also detect any nucleosomes potentially positioned in this *MAT* region and could be misinterpreted as nucleosomal positioning at *HML*. Note that one of the primers designed to detect the L6 nucleosome position at *HML* is homologous to Yα, so *MAT***a** sequences will not be amplified. From a similar analysis of a *MAT***a** *hml*Δ *hmr*Δ strain (JKM139), we conclude that the *MAT***a** Z1–Z2 region is much less well protected than *HML* (Fig. S2), with ≈40% of total L5 protection attributable to nucleosomes at *MAT***a**. The presence of protected sequences at *MAT* is only likely to affect the MNase protection profile before HO induction, because nucleosomes at *MAT* have been shown to be quickly remodeled or removed after DSB formation (22, 57–59). It is possible that RPA-bound ssDNA or Rad51-ssDNA filament formed at *MAT* could afford some level of MNase protection, but our observation that L5–L6 internucleosomal sequences show a >70% reduction in MNase protection argues against this idea (Fig. 6*B*).

Unexpectedly, nucleosome remodeling within *HML* is very limited during a *MAT* switch, although maximal nucleosome remodeling correlates with maximal *MAT-HML* synapsis (Fig. 6*B*). This suggests that changes in MNase protection require Rad51-mediated pairing of homologous sequences. Nucleosome remodeling seems to be a coordinated phenomenon: nucleosomes L5–L10 all showed decreased MNase protection to the same extent at 75 min, the time with the greatest MNase sensitivity (Fig. 6*B*). Loss of protection at these different nucleosomes proceeded with similar kinetics (Fig. S3*A*). It is interesting that nucleosomes in Yα are changing before initiation of DNA synthesis. This could occur if strand invasions create extended D-loop structures; we are currently testing this possibility. The decrease in MNase protection during *MAT* switching is specific to *HML*, as indicated by a lack of nucleosome remodeling within a centromeric region (Fig. S2*B*).

The relatively low level of nucleosome remodeling is unexpected if it is necessary to establish accessibility of the synapsed 3′ end of the invading *MAT* ssDNA to recruit replication machinery required to initiate DNA synthesis. The modest changes in nucleosome protection could be explained if the repair process quickly becomes asynchronous within a switching population in all cell cycle phases. It is also possible that nucleosome remodeling is a transient process, especially if one considers the model in which strand invasion and subsequent DNA synthesis occurs in a migrating D-loop (60, 61). In this situation, nucleosomes could reassemble as soon as donor duplex DNA is reformed.

In an attempt to increase repair synchrony at the strand invasion step, we replaced *HML W* and *X* regions with a *URA3* gene to remove all homology to the left side of *MAT* such that an HO-induced DSB at *MAT* could only be repaired by BIR (Fig. 6*C*). This modification did not alter the heterochromatic state of *HML* because these cells were Ura$^-$ unless desilenced by nicotinamide addition (62). We previously showed that initiation of DNA replication by BIR is delayed several hours compared with GC (63, 64), thus a much larger proportion of the population should be in a remodeled chromatin state, awaiting initiation of new DNA synthesis. Interestingly, *MAT*-BIR primer extension kinetics were almost identical to those of a typical *MAT* switch; however, *MAT*-BIR product formation was significantly delayed (Fig. S4). Changes in MNase protection levels at *HML*α(ΔW/X) during *MAT*-BIR indicate that alterations in heterochromatic nucleosomes are more extensive or else occur in a larger proportion of cells than during normal *MAT* switching (Fig. 6*C*). On average, nucleosomes L5–L10 become 38.0% ± 7.1% (95% confidence interval; $P < 0.0003$, *t* test) more susceptible to MNase digestion during *MAT*-BIR than during normal *MAT* switching. The spike in MNase protection of the L6 nucleosome 45 min after HO induction observed for both *MAT* switching and *MAT*-BIR coincides with initial detection of *MAT-HML* synapsis, suggesting that the Rad51 nucleoprotein filament may initially impart MNase protection within this region before nucleosome remodeling. *MAT*-BIR results in a greater loss of MNase protection

within the region containing L6–L10 nucleosomes, and maximal deprotection occurs at $t = 120$ min, 45 min later than during *MAT* switching (Fig. 6*E*). At 60 min the extent of MNase protection in *MAT* switching and *MAT*-BIR were comparable, and by 90 min nucleosome remodeling during *MAT*-BIR had begun to surpass *MAT* switching. As with *MAT* switching, nucleosome remodeling during *MAT*-BIR was a coordinated phenomenon because all nucleosomes (L5–L10) were remodeled with similar kinetics (Fig. S3*B*).

The increased and sustained chromatin remodeling observed during *MAT*-BIR provided an excellent opportunity to study the role of chromatin remodelers during HR; to this end we deleted Rad54. We previously showed that, without Rad54, new DNA synthesis is prevented during DSB repair (23), so there should not be the flux of different chromatin states that may occur in the WT BIR context. We and others have shown that Rad54 is not required for strand invasion at *HML*, although the efficiency or stability of Rad51 association with *HML* was notably lower in *rad54*Δ cells (23, 51). In our *MAT*-BIR experiments both WT and *rad54*Δ cells exhibited similar *MAT-HML* synapsis (Fig. 6*D*). Without Rad54, some nucleosome remodeling does occur during *MAT*-BIR repair, but these changes were delayed 2 h compared with WT *MAT*-BIR and were confined to the L5 and L6 nucleosomes (Fig. 6*D*). The extent of nucleosome remodeling within the region protected by the L5 and L6 nucleosomes observed in *rad54*Δ cells was similar to WT (Fig. 6*E*), indicating that the Rad51 filament may be capable of destabilizing nucleosomes as homologous *MAT* and *HML* sequences interact. In the absence of Rad54 some internucleosomal regions actually exhibited an increase in MNase protection (Fig. 6*E*). Together these data suggest that Rad54 plays an important role for remodeling donor chromatin after Rad51-mediated synapsis, although it is not necessary for synapsis.

Discussion

By analyzing *MAT* switching in 10-min intervals, we have provided a high-resolution picture of the DSB repair mechanism, SDSA. We confirmed our earlier finding that Rad51 is loaded on DSB ends within 30 min of DSB formation (22). These previous results showed that 5′ to 3′ resection must also begin very rapidly, because ssDNA binding protein complex, RPA, is detected by ChIP coincident with DSB formation.

Searching for homologous sequences located 200 kb away on the same chromosome proved to be surprisingly faster than previously appreciated. Rad51 became associated with *HML* donor sequences only 10 min after filament formation at *MAT*. It is likely that the interaction between *HML* and *MAT* is unusually efficient, because their recombination is facilitated by a cis-acting recombination enhancer (RE) (15, 65–67). We believe that RE acts by recruiting proteins that in turn bind to DSB-induced chromatin modifications in the vicinity of a DSB, thus bringing *HML* into close proximity to the homology-searching Rad51 filament. It is quite likely that other searches without RE, between chromosomes as well as intrachromosomally, take substantially more time to locate very small amounts of homology (327 bp for Z1/Z2) against a background of more than 10 Mb of chromosomal DNA.

The early association we see between Rad51 and the donor does not imply that this initial encounter will invariably lead to a stable strand invasion structure. There are several reasons why the Rad51 filament may initially form paranemic, side-by-side base pairings rather than a fully interwound plectonemic strand exchange. This would enable the process to be transiently reversible. Thus, if a DSB in a repeated sequence led to the situation whereby each Rad51-coated end collided with a different repeat (one with *HMR* and one with *HML*, for example), a delay in forming stable structures could allow one or both ends to dissociate and make another attempt to find homology. Indeed this step seems to be regulated in budding yeast by the recombination execution checkpoint (REC), which delays initiation of new DNA synthesis (and possibly plectonemic strand invasion structures) until both ends of a DSB are engaged on the same template (63).

Strand Invasion and Chromatin Remodeling. Successful strand invasion involves not simply the challenge of the Rad51 nucleoprotein filament searching for a short region of homology; the search takes place in the context of chromatin. This problem is especially acute when *MAT* sequences must find and invade homologous sequences in highly positioned nucleosomes at *HML* or *HMR*. Here we have been able to visualize changes in nucleosome positioning/occupancy during strand invasion. These changes seem to be quite transient in populations capable of quickly initiating new DNA synthesis but can be maintained for a longer period when initiating new DNA synthesis is delayed by the REC where only one side of the DSB shares homology to donor sequences. Still, loss of MNase protection is only partial, with approximately 40% of the initial level remaining. This could reflect the idea that strand invasion is a reversible step until there is some sort of "commitment" to initiating new DNA synthesis. Strand invasion reversibility might be tied to the action of Mph1 and Srs2 helicases, both of which play key roles during SDSA. It is also possible the Rad51 filament adds some protection against MNase digestion, but there is no equivalent increased protection in the L5–L6 internucleosomal region. This lack of increased protection between nucleosomes also suggests that nucleosomes are not repositioned by simply sliding.

A very important finding was the lack of nucleosome displacement in *rad54*Δ cells even though Rad51 efficiently associated with *HML*. Rad54 has been suggested both to promote plectonemic interwinding of the invading strand as well as to displace Rad51 from the 3′ end of the invading strand to facilitate recruitment of DNA polymerase (53, 68). The results we present here suggest that Rad54 is required before replication machinery recruitment, namely remodeling nucleosomes within the donor locus. It should now be possible to ask about the roles of other chromatin remodeling complexes in strand invasion.

Initiation of New DNA Synthesis. There is a striking 40-min delay between initial detection of Rad51-mediated strand exchange and observable primer extension initiation. Some of this delay may reflect the reversible nature of the initial Rad51 filament-donor encounter, although a significant part of this delay may arise from the need to assemble a DNA replication complex in the absence of proteins typically required to initiate replication at origins. Indeed, many proteins required to open up origins, assemble DNA polymerases, and aid in subsequent strand copying are not required for *MAT* switching, including Mcm2-7/GINS/Cdc45 helicase proteins and Cdc7 kinase (32). However, as we show here, Dpb11, a key player during normal DNA replication at the preloading complex step along with Polε and GINS complex, is clearly required during *MAT* switching. However, we know that GINS is not required and Polε is dispensable, because a temperature-sensitive mutation of Polε is still able to switch, presumably by recruiting Polδ (33). Precisely how Dpb11 works in DSB repair remains to be elucidated.

One of the striking findings about *MAT* switching is that the DNA copying process exhibits a 1,400-fold increase in mutation rate (34, 69). Many of these events are best explained by dissociation of the nascent strand from its template, despite the presence of PCNA, leading to several characteristic mutations: −1 frame shifts, complex events mediated by quasipalindrome formation on the partially replicated strand, and even interchromosomal template switches (34). We note that a similar low DNA polymerase processivity has been suggested from DSB repair in *Drosophila* (70).

Previously White and Haber (18), using a plasmid-based HO system, found that there was a 30-min delay between new DNA synthesis initiation and *MAT* switching completion. Here, in a situation whereby *GAL::HO* is chromosomally integrated and virtually all cells form a DSB, we did not observe this delay. This was confirmed by assaying the appearance of the *MAT*-X-Yα

junction (Fig. S5). Whether this PCR assay detects primer extension off the 3′ end of the DSB left side using *HML* W/X as a template, or the completion of *MAT* switching itself, cannot be determined. Regardless, coincident appearance of this PCR product with product assayed by Southern blot indicates that these later *MAT* switching steps occur in rapid succession. The difference between White and Haber (18) and the results reported here may stem from the fact that White and Haber analyzed these steps in synchronized cells, released from α-factor–induced G1 arrest, whereas the assays reported here were carried out on cycling cells.

Nonhomologous Tail Removal and Later Steps in Repair. In the asynchronous cells used in our experiments, joining of the left side of the break (W/X) to Yα donor sequences becomes apparent at 70 min, the same time we observe primer extension from the Z end. It is not clear whether the initial PCR product that detects this joining represents strand invasion of the left end into the donor or whether it arises from primer extension of the left end after annealing to the displaced first strand. In either case, **Ya** sequences at the end of the DSB must be removed before the W/X 3′ end can be extended into Yα. A key question is when removal of the NH-3′ ended tail occurs. Our observation that NH-tail clipping is nearly eliminated in *rad54*Δ cells (Fig. 5) could mean that tail clipping occurs after new DNA synthesis has extended the first end, allowing annealing to the second end that did not necessarily invade the donor, but because *rad54*Δ also fails to promote nucleosome displacement during strand invasion it is also possible that synapsis of the W/X region with the donor does not provide a sufficiently stable structure to promote tail clipping by Rad1–Rad10 and its associated factors. Interactions between homologous sequences within topologically constrained dsDNA and ssDNA containing NH-tails have been shown to be unstable, likely owing to an inability to form plectonemic structures (44–46). We conclude that 3′ tail removal most likely depends on new DNA synthesis from the end with perfect homology to provide a new strand that can pair with and promote tail clipping when the free ends are not constrained to intertwine, as in strand annealing.

Known Unknowns of *MAT* Switching in Budding Yeast. There are still many steps in the process of DSB repair by GC that need to be explored. Exactly what happens to the nucleosomes harboring donor DNA during strand invasion? Similarly, how are nucleosomes reestablished at *MAT* after repair is complete? We recently showed that repair can be completed in the absence of known histone H3 chaperones, Asf1, and the chromatin assembly factor (CAF) complex (71), but if the process is slow enough to trigger cell cycle arrest by the DNA damage checkpoint (e.g., in interchromosomal HR), then cells lacking these chaperones are unable to resume cell cycle progression. This result suggests these chaperones play a role in chromatin reassembly; but to look at this we will need a *MAT* locus with better-positioned nucleosomes that will at the same time not prevent HO cleavage. Moreover, we still need a full accounting of the proteins required to initiate new DNA synthesis and an understanding of the kinetics and order of assembly of these factors at the D-loop.

Another mystery concerns the specific roles of both Srs2 and Mph1 helicases during SDSA. The absence of Srs2 causes a marked reduction in successful recombination, whereas loss of Mph1 seems to channel most DSB repair events into an alternative DSB repair process including formation of dHJs and the possibility of GC associated with COs (72). Both of these helicases have been implicated in preventing formation or dismantling D-loops, but do they also play a role in unwinding newly synthesized DNA from its template, and would nucleosome rearrangements of the donor be affected by deleting them?

Studying Recombination Events in Detail in Other Eukaryotes. The use of site-specific endonucleases to create a large enough population of cells undergoing synchronous repair to monitor in ways that have been so successful in budding yeast has yet to be accomplished, although DSBs have been induced by HO or I-SceI enzymes in fission yeast, fruit flies, and mammalian cells (73–75). The excision of transposable elements has also been used, but again not with the kind of synchrony required for physical monitoring of repair (70, 76). Use of steroid-regulated I-SceI has shown potential to create a DSB synchronously (77). Interestingly, a recent study using electroporation of linearized dsDNA into mammalian cells that contain a homologous chromosomal donor found nascent DNA formed by polymerizing 3′ ends of invading strands within 30 min (78), which is actually faster than we see in budding yeast. It will be necessary to develop more synchronous HR systems in higher organisms to better compare the mechanism of DSB repair in budding yeast and more complex eukaryotes.

Materials and Methods

Strains and molecular methods used to analyze recombination are detailed in *SI Materials and Methods*. The methods used to monitor *MAT* switching by Southern blot, PCR, and ChIP have been previously described (22, 23). Monitoring removal of NH-ssDNA tails from DSB ends was based on methods described previously (79). Chromatin analysis by MNase was based on methods described previously (54).

ACKNOWLEDGMENTS. We thank M. Lichten, G. Ira, S. E. Lee, and J.-A. Kim for helpful comments on this article. The work described in this article is built on a foundation of contributions from more than 50 graduate students, postdoctoral fellows, and technicians who have worked in the J.E.H. laboratory. Key contributions in understanding HO endonuclease-mediated recombination and repair were made by Michael Lichten, Rhona Borts, Lance Davidow, Charles White, Bernadette Connolly, Norah Rudin, Jacqueline Fishman-Lobell, Evgeny Ivanov, Kent Moore, Sang-Eun Lee, Xiaohua Wu, Cherry Wu, Kaiming Sun, Giovanni Bosco, Allyson Holmes, Frédéric Pâques, Guy-Franck Richard, Mónica Colaiàcovo, Moreshwar Vaze, Anna Malkova, Grzgorz Ira, Maria Valencia, Xuan Wang, Eric Coïc, Jung-Ae Kim, John Lydeard, Suvi Jain, and Neal Sugawara, who has worked on these projects for almost 20 years. This work has been supported by National Institutes of Health Grants GM20056, GM61766, GM76020, 2T32GM007122, and earlier grants from the National Science Foundation and Department of Energy.

1. Sonoda E, et al. (1998) Rad51-deficient vertebrate cells accumulate chromosomal breaks prior to cell death. *EMBO J* 17:598–608.
2. Moore JK, Haber JE (1996) Cell cycle and genetic requirements of two pathways of nonhomologous end-joining repair of double-strand breaks in *Saccharomyces cerevisiae*. *Mol Cell Biol* 16:2164–2173.
3. Ma JL, Kim EM, Haber JE, Lee SE (2003) Yeast Mre11 and Rad1 proteins define a Ku-independent mechanism to repair double-strand breaks lacking overlapping end sequences. *Mol Cell Biol* 23:8820–8828.
4. Symington LS (2002) Role of RAD52 epistasis group genes in homologous recombination and double-strand break repair. *Microbiol Mol Biol Rev* 66:630–670.
5. Zinn AR, Pohlman JK, Perlman PS, Butow RA (1988) In vivo double-strand breaks occur at recombinogenic G + C-rich sequences in the yeast mitochondrial genome. *Proc Natl Acad Sci USA* 85:2686–2690.
6. Borts RH, Lichten M, Hearn M, Davidow LS, Haber JE (1984) Physical monitoring of meiotic recombination in *Saccharomyces cerevisiae*. *Cold Spring Harb Symp Quant Biol* 49:67–76.
7. Rudin N, Haber JE (1988) Efficient repair of HO-induced chromosomal breaks in *Saccharomyces cerevisiae* by recombination between flanking homologous sequences. *Mol Cell Biol* 8:3918–3928.
8. Fishman-Lobell J, Rudin N, Haber JE (1992) Two alternative pathways of double-strand break repair that are kinetically separable and independently modulated. *Mol Cell Biol* 12:1292–1303.
9. Plessis A, Perrin A, Haber JE, Dujon B (1992) Site-specific recombination determined by I-SceI, a mitochondrial group I intron-encoded endonuclease expressed in the yeast nucleus. *Genetics* 130:451–460.
10. Connolly B, White CI, Haber JE (1988) Physical monitoring of mating type switching in *Saccharomyces cerevisiae*. *Mol Cell Biol* 8:2342–2349.
11. Stone EM, Pillus L (1998) Silent chromatin in yeast: an orchestrated medley featuring Sir3p [corrected]. *Bioessays* 20:30–40.
12. Lustig AJ (1998) Mechanisms of silencing in *Saccharomyces cerevisiae*. *Curr Opin Genet Dev* 8:233–239.
13. Ercan S, Simpson RT (2004) Global chromatin structure of 45,000 base pairs of chromosome III in a- and alpha-cell yeast and during mating-type switching. *Mol Cell Biol* 24:10026–10035.
14. Klar AJ, Hicks JB, Strathern JN (1982) Directionality of yeast mating-type interconversion. *Cell* 28:551–561.
15. Wu X, Haber JE (1996) A 700 bp cis-acting region controls mating-type dependent recombination along the entire left arm of yeast chromosome III. *Cell* 87:277–285.

16. Wu X, Moore JK, Haber JE (1996) Mechanism of MAT alpha donor preference during mating-type switching of *Saccharomyces cerevisiae*. *Mol Cell Biol* 16:657–668.
17. Herskowitz I, Jensen RE (1991) Putting the HO gene to work: Practical uses for mating-type switching. *Methods Enzymol* 194:132–146.
18. White CI, Haber JE (1990) Intermediates of recombination during mating type switching in *Saccharomyces cerevisiae*. *EMBO J* 9:663–673.
19. Fishman-Lobell J, Haber JE (1992) Removal of nonhomologous DNA ends in double-strand break recombination: The role of the yeast ultraviolet repair gene RAD1. *Science* 258:480–484.
20. Ira G, et al. (2004) DNA end resection, homologous recombination and DNA damage checkpoint activation require CDK1. *Nature* 431:1011–1017.
21. Aylon Y, Kupiec M (2005) Cell cycle-dependent regulation of double-strand break repair: A role for the CDK. *Cell Cycle* 4:259–261.
22. Wang X, Haber JE (2004) Role of *Saccharomyces* single-stranded DNA-binding protein RPA in the strand invasion step of double-strand break repair. *PLoS Biol* 2:E21.
23. Sugawara N, Wang X, Haber JE (2003) In vivo roles of Rad52, Rad54, and Rad55 proteins in Rad51-mediated recombination. *Mol Cell* 12:209–219.
24. Wolner B, van Komen S, Sung P, Peterson CL (2003) Recruitment of the recombinational repair machinery to a DNA double-strand break in yeast. *Mol Cell* 12: 221–232.
25. Meselson M, Stahl FW (1958) The replication of DNA in *Escherichia coli*. *Proc Natl Acad Sci USA* 44:671–682.
26. Ira G, Satory D, Haber JE (2006) Conservative inheritance of newly synthesized DNA in double-strand break-induced gene conversion. *Mol Cell Biol* 26:9424–9429.
27. Pâques F, Haber JE (1999) Multiple pathways of recombination induced by double-strand breaks in *Saccharomyces cerevisiae*. *Microbiol Mol Biol Rev* 63:349–404.
28. Haber JE, Rogers DT, McCusker JH (1980) Homothallic conversions of yeast mating-type genes occur by intrachromosomal recombination. *Cell* 22:277–289.
29. Strathern JN, Newlon CS, Herskowitz I, Hicks JB (1979) Isolation of a circular derivative of yeast chromosome III: Implications for the mechanism of mating type interconversion. *Cell* 18:309–319.
30. Hawthorne DC (1963) A deletion in yeast and its bearing on the structure of the mating type locus. *Genetics* 48:1727–1729.
31. Bzymek M, Thayer NH, Oh SD, Kleckner N, Hunter N (2010) Double Holliday junctions are intermediates of DNA break repair. *Nature* 464:937–941.
32. Lydeard JR, et al. (2010) Break-induced replication requires all essential DNA replication factors except those specific for pre-RC assembly. *Genes Dev* 24: 1133–1144.
33. Wang X, et al. (2004) Role of DNA replication proteins in double-strand break-induced recombination in *Saccharomyces cerevisiae*. *Mol Cell Biol* 24:6891–6899.
34. Hicks WM, Kim M, Haber JE (2010) Increased mutagenesis and unique mutation signature associated with mitotic gene conversion. *Science* 329:82–85.
35. Masumoto H, Sugino A, Araki H (2000) Dpb11 controls the association between DNA polymerases alpha and epsilon and the autonomously replicating sequence region of budding yeast. *Mol Cell Biol* 20:2809–2817.
36. Holmes AM, Haber JE (1999) Double-strand break repair in yeast requires both leading and lagging strand DNA polymerases. *Cell* 96:415–424.
37. Araki H, Leem SH, Phongdara A, Sugino A (1995) Dpb11, which interacts with DNA polymerase II(epsilon) in *Saccharomyces cerevisiae*, has a dual role in S-phase progression and at a cell cycle checkpoint. *Proc Natl Acad Sci USA* 92:11791–11795.
38. McCulloch RD, Read LR, Baker MD (2003) Strand invasion and DNA synthesis from the two 3′ ends of a double-strand break in Mammalian cells. *Genetics* 163:1439–1447.
39. Lyndaker AM, Goldfarb T, Alani E (2008) Mutants defective in Rad1-Rad10-Slx4 exhibit a unique pattern of viability during mating-type switching in *Saccharomyces cerevisiae*. *Genetics* 179:1807–1821.
40. Ivanov EL, Haber JE (1995) RAD1 and RAD10, but not other excision repair genes, are required for double-strand break-induced recombination in *Saccharomyces cerevisiae*. *Mol Cell Biol* 15:2245–2251.
41. Sugawara N, Pâques F, Colaiácovo M, Haber JE (1997) Role of *Saccharomyces cerevisiae* Msh2 and Msh3 repair proteins in double-strand break-induced recombination. *Proc Natl Acad Sci USA* 94:9214–9219.
42. Flott S, et al. (2007) Phosphorylation of Slx4 by Mec1 and Tel1 regulates the single-strand annealing mode of DNA repair in budding yeast. *Mol Cell Biol* 27:6433–6445.
43. Li F, et al. (2008) Microarray-based genetic screen defines SAW1, a gene required for Rad1/Rad10-dependent processing of recombination intermediates. *Mol Cell* 30: 325–335.
44. Bianchi M, DasGupta C, Radding CM (1983) Synapsis and the formation of paranemic joints by *E. coli* RecA protein. *Cell* 34:931–939.
45. Christiansen G, Griffith J (1986) Visualization of the paranemic joining of homologous DNA molecules catalyzed by the RecA protein of *Escherichia coli*. *Proc Natl Acad Sci USA* 83:2066–2070.
46. Riddles PW, Lehman IR (1985) The formation of paranemic and plectonemic joints between DNA molecules by the recA and single-stranded DNA-binding proteins of *Escherichia coli*. *J Biol Chem* 260:165–169.
47. Namsaraev EA, Berg P (2000) Rad51 uses one mechanism to drive DNA strand exchange in both directions. *J Biol Chem* 275:3970–3976.
48. Gupta RC, Golub EI, Wold MS, Radding CM (1998) Polarity of DNA strand exchange promoted by recombination proteins of the RecA family. *Proc Natl Acad Sci USA* 95: 9843–9848.
49. McGill C, Shafer B, Strathern J (1989) Coconversion of flanking sequences with homothallic switching. *Cell* 57:459–467.
50. Weiffenbach B, Haber JE (1985) Homothallic switching of *Saccharomyces cerevisiae* mating type genes by using a donor containing a large internal deletion. *Mol Cell Biol* 5:2154–2158.
51. Wolner B, Peterson CL (2005) ATP-dependent and ATP-independent roles for the Rad54 chromatin remodeling enzyme during recombinational repair of a DNA double strand break. *J Biol Chem* 280:10855–10860.
52. Houston PL, Broach JR (2006) The dynamics of homologous pairing during mating type interconversion in budding yeast. *PLoS Genet* 2:e98.
53. Sinha M, Peterson CL (2008) A Rad51 presynaptic filament is sufficient to capture nucleosomal homology during recombinational repair of a DNA double-strand break. *Mol Cell* 30:803–810.
54. Sekinger EA, Moqtaderi Z, Struhl K (2005) Intrinsic histone-DNA interactions and low nucleosome density are important for preferential accessibility of promoter regions in yeast. *Mol Cell* 18:735–748.
55. Yuan GC, et al. (2005) Genome-scale identification of nucleosome positions in *S. cerevisiae*. *Science* 309:626–630.
56. Weiss K, Simpson RT (1998) High-resolution structural analysis of chromatin at specific loci: *Saccharomyces cerevisiae* silent mating type locus HMLalpha. *Mol Cell Biol* 18: 5392–5403.
57. Shim EY, et al. (2007) RSC mobilizes nucleosomes to improve accessibility of repair machinery to the damaged chromatin. *Mol Cell Biol* 27:1602–1613.
58. Kent NA, Chambers AL, Downs JA (2007) Dual chromatin remodeling roles for RSC during DNA double strand break induction and repair at the yeast MAT locus. *J Biol Chem* 282:27693–27701.
59. Chung WH, Zhu Z, Papusha A, Malkova A, Ira G (2010) Defective resection at DNA double-strand breaks leads to de novo telomere formation and enhances gene targeting. *PLoS Genet* 6:e1000948.
60. Ferguson DO, Holloman WK (1996) Recombinational repair of gaps in DNA is asymmetric in *Ustilago maydis* and can be explained by a migrating D-loop model. *Proc Natl Acad Sci USA* 93:5419–5424.
61. Formosa T, Alberts BM (1986) DNA synthesis dependent on genetic recombination: Characterization of a reaction catalyzed by purified bacteriophage T4 proteins. *Cell* 47:793–806.
62. Bitterman KJ, Anderson RM, Cohen HY, Latorre-Esteves M, Sinclair DA (2002) Inhibition of silencing and accelerated aging by nicotinamide, a putative negative regulator of yeast sir2 and human SIRT1. *J Biol Chem* 277:45099–45107.
63. Jain S, et al. (2009) A recombination execution checkpoint regulates the choice of homologous recombination pathway during DNA double-strand break repair. *Genes Dev* 23:291–303.
64. Malkova A, Naylor ML, Yamaguchi M, Ira G, Haber JE (2005) RAD51-dependent break-induced replication differs in kinetics and checkpoint responses from RAD51-mediated gene conversion. *Mol Cell Biol* 25:933–944.
65. Coïc E, Sun K, Wu C, Haber JE (2006) Cell cycle-dependent regulation of *Saccharomyces cerevisiae* donor preference during mating-type switching by SBF (Swi4/Swi6) and Fkh1. *Mol Cell Biol* 26:5470–5480.
66. Sun K, Coïc E, Zhou Z, Durrens P, Haber JE (2002) *Saccharomyces* forkhead protein Fkh1 regulates donor preference during mating-type switching through the recombination enhancer. *Genes Dev* 16:2085–2096.
67. Ruan C, Workman JL, Simpson RT (2005) The DNA repair protein yKu80 regulates the function of recombination enhancer during yeast mating type switching. *Mol Cell Biol* 25:8476–8485.
68. Li X, Heyer WD (2009) RAD54 controls access to the invading 3′-OH end after RAD51-mediated DNA strand invasion in homologous recombination in *Saccharomyces cerevisiae*. *Nucleic Acids Res* 37:638–646.
69. Rattray AJ, Shafer BK, McGill CB, Strathern JN (2002) The roles of REV3 and RAD57 in double-strand-break-repair-induced mutagenesis of *Saccharomyces cerevisiae*. *Genetics* 162:1063–1077.
70. McVey M, Adams M, Staeva-Vieira E, Sekelsky JJ (2004) Evidence for multiple cycles of strand invasion during repair of double-strand gaps in *Drosophila*. *Genetics* 167: 699–705.
71. Kim JA, Haber JE (2009) Chromatin assembly factors Asf1 and CAF-1 have overlapping roles in deactivating the DNA damage checkpoint when DNA repair is complete. *Proc Natl Acad Sci USA* 106:1151–1156.
72. Prakash R, et al. (2009) Yeast Mph1 helicase dissociates Rad51-made D-loops: implications for crossover control in mitotic recombination. *Genes Dev* 23:67–79.
73. Cullen JK, et al. (2007) Break-induced loss of heterozygosity in fission yeast: Dual roles for homologous recombination in promoting translocations and preventing de novo telomere addition. *Mol Cell Biol* 27:7745–7757.
74. Rong YS, Golic KG (2003) The homologous chromosome is an effective template for the repair of mitotic DNA double-strand breaks in *Drosophila*. *Genetics* 165: 1831–1842.
75. Weinstock DM, Nakanishi K, Helgadottir HR, Jasin M (2006) Assaying double-strand break repair pathway choice in mammalian cells using a targeted endonuclease or the RAG recombinase. *Methods Enzymol* 409:524–540.
76. Nassif N, Penney J, Pal S, Engels WR, Gloor GB (1994) Efficient copying of nonhomologous sequences from ectopic sites via P-element-induced gap repair. *Mol Cell Biol* 14:1613–1625.
77. Soutoglou E, et al. (2007) Positional stability of single double-strand breaks in mammalian cells. *Nat Cell Biol* 9:675–682.
78. Si W, et al. (2010) A strand invasion 3′ polymerization intermediate of mammalian homologous recombination. *Genetics* 185:443–457.
79. Toh GW, et al. (2010) Mec1/Tel1-dependent phosphorylation of Slx4 stimulates Rad1-Rad10-dependent cleavage of non-homologous DNA tails. *DNA Repair (Amst)* 9: 718–726.